PERGAMON

Available online at www.sciencedirect.com

SCIENCE DIRECT®

Polyhedron 22 (2003) 247–255

POLYHEDRON

www.elsevier.com/locate/poly

Copper(I)–azoimidazoles: a comparative account on the structure and electronic properties of copper(I) complexes of 1-methyl-2-(phenylazo)imidazole and 1-alkyl-2-(naphthyl-(α/β)-azo)imidazoles

Joydev Dinda[a], Umasankar Ray[a], Golam Mostafa[b], Tian-Huey Lu[b], Anwar Usman[c], Ibrahim Abdul Razak[c], Suchada Chantrapromma[c,d], Hoong-Kun Fun[c], Chittaranjan Sinha[a,*]

[a] *Department of Chemistry, The University of Burdwan, Burdwan 713104, India*
[b] *Department of Physics, National Tsing-Hua University, Hsinchu 300, Taiwan, ROC*
[c] *School of Physics, University Sains Malaysia, 11800 USM, Penang, Malaysia*
[d] *Department of Chemistry, Prince of Songkla University, Hat-Yai, Songkhla 90112, Thailand*

Received 15 May 2002; accepted 10 October 2002

Abstract

Bis-[1-alkyl-2-(naphthyl-(α/β)azo)imidazole]copper(I) perchlorate derivatives, [Cu(α-NaiR)$_2$(ClO$_4$)] and Cu(β-NaiR)$_2$](ClO$_4$), have been characterised by spectral and electrochemical studies. The single crystal X-ray structure of bis-[1-ethyl-2-(naphthyl-α-azo)imidazole]copper(I) perchlorate shows strong bonding with two imidazole-N atoms, two azo-N donors interact weakly and the structure is described as having a [2+2] distorted linear geometry. A structural comparison has been done with the X-ray structure of bis-[1-methyl-2-(phenylazo)imidazole]copper(I) perchlorate which is T_d symmetric. Solution electronic spectra and redox properties are compared and have been correlated with EHMO calculation.

Keywords: Naphthylazoimidazoles; Copper(I) complexes; X-ray structures; Electrochemistry; EHMO

1. Introduction

A correlation between the structures and electronic configuration with chemical, electrochemical, photophysical/photochemical properties of molecules is the origin of great interest to design molecules of specific interest. Calculation on molecules in a theoretically consistent framework and correlation with their properties allow a convenient way to understand about these molecules and their respective homologues [1–11]. The EHMO theory has now come into the age. It is used to enable us to understand a wide range of physical properties of molecules, their reactivity and the pathways taken by chemical reactions [8,9]. Use of structural parameters from single crystal X-ray diffraction data in the EHMO calculation is now widely accepted [12–15]. An experimentalist thus can understand why molecules of concern react the way they do, on the basis of EHMO calculation. In our group of recent publications [13–15] we have reported a correlation between theoretically calculated energy levels by the EHMO theory and the spectral and electrochemical properties of transition metal complexes of arylazoheterocycles.

In arylazoheterocycles the chromophore is the azoimine function, –N=N–C=N–, which is π-acidic and stabilises low valent metal redox state such as Cu(I), Ru(II). The π-acidity of the function is largely dependent on the nature of the heterocycle and aryl group. A significant effect is observed [16] on changing from a five to six member heterocycle, increasing the number of heteroatoms and substituting an aryl group by a naphthyl group. The naphthyl group provides a greater steric crowding, more reactivity and better electron

---

* Corresponding author. Tel.: +91-342-55-7683; fax: +91-342-53-0452
E-mail address: c_r_sinha@yahoo.com (C. Sinha).

PII: S0277-5387(02)01341-4

donating property than that of a phenyl ring in a competitive environment [17–20].

The affinity of the azoimine function to stabilise Cu(I) (d^{10}) oxidation state has led us to synthesise high potential copper(I) complexes of arylazoheterocycles [21–23]. It has been proposed that the stability, high intense UV–Vis spectra and high electrochemical potential of the Cu(II)/Cu(I) couple are due to a strong charge transfer transition from d_π (Cu(I)) → π* (ligand) orbitals. In this article we demonstrate the structural differences between copper(I) complexes of 1-methyl-2-(phenylazo)imidazole (PaiMe) and 1-alkyl-2-(naphthyl-α/β-azo)imidazoles (α/β-NaiR) (Scheme 1). Detailed synthesis, spectral studies and electrochemical properties of [Cu(α/β-NaiR)$_2$](ClO$_4$) are also reported. The properties have been correlated with EHMO calculations.

2. Experimental

2.1. Materials

The synthesis and spectral measurements of bis-[1-methyl-2-(phenylazo)imidazole]copper(I) perchlorate were reported elsewhere [21]. 1-Alkyl-2-(naphthylazo)imidazoles were also prepared by known procedures [17,18]. The purification/preparation of solvents and supporting electrolyte, [Bu$_4$N][ClO$_4$], were carried out as previously reported [13]. Dinitrogen was purified by bubbling through an alkaline pyrogallol solution. All other chemicals and solvents were reagent grade and were used as received.

2.2. Physical measurements

Microanalytical (C, H, N) data were obtained from a Perkin–Elmer 2400 CHNS/O elemental analyser. Spectroscopic data were obtained using the following instruments: UV–Vis, JASCO UV–Vis/NIR model V-570; IR (KBr disk, 4000–200 cm^{-1}), JASCO FT-IR model 420 spectrophotometer and ^{1}H NMR, Bruker 300 MHz FT-NMR spectrometer. Electrochemical experiments were carried out using an EG & G PARC model 270 electrochemical instrument. The reported potentials are uncorrected for junction potential.

2.3. Synthesis of bis-[1-ethyl-2-(naphthyl-α-azo)imidazole]copper(I) perchlorate

The ligand 1-ethyl-2-(naphthyl-α-azo)imidazole (0.50 g, 2 mmol) in dry MeOH (25 ml) was added to a methanolic solution (20 ml) of [Cu(MeCN)$_4$][ClO$_4$] (0.30 g, 0.92 mmol) in a nitrogen atmosphere at room temperature (r.t.). The dark-brown solution was stirred for 3 h. The solution was reduced to half of its original volume by bubbling nitrogen gas through it, a brown–red crystalline precipitate appeared which was filtered, washed with methanol–water (1:1, v/v) and dried over CaCl$_2$. The dried compound was purified by column chromatography. To a column of silica gel (60–120 mesh), prepared in benzene, a chloroform solution of the complex was eluted first by chloroform and a light-red band was rejected. The desired deep brown–red band was collected by elution using a methanol–chloroform (4:1, v/v) mixture and evaporated slowly in air. The yield was 0.39 g (64%). The microanalytical data of the complex is as follows, [Cu(α-NaiEt)$_2$](ClO$_4$) (**2b**): *Anal.* Found: C, 54.2; H, 4.1; N, 15.9, Cu, 9.6. Calc. for $C_{30}H_{28}N_8ClO_4Cu$: C, 53.9; H, 4.2; N, 16.1; Cu, 9.4%.

All other complexes were prepared following identical procedures with yields of 55–70% and microanalytical data of the complexes are as follows, [Cu(α-NaiMe)$_2$](ClO$_4$) (**2a**): *Anal.* Found: C, 51.7; H, 3.8, N, 17.1, Cu, 10.0. Calc. for $C_{28}H_{24}N_8ClO_4Cu$: C, 52.0; H, 3.6, N, 17.3; Cu, 9.8%. [Cu(α-NaiBz)$_2$](ClO$_4$) (**2c**): *Anal.* Found: C, 56.9; H, 4.1; N, 14.2; Cu, 8.1. Calc. for

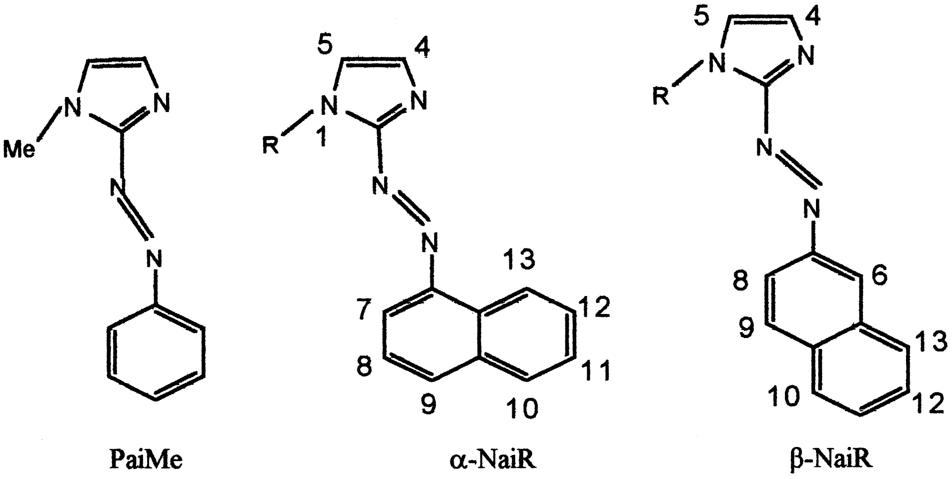

Scheme 1. Chemical structure of PaiMe, α-NaiR, and β-NaiR.

$C_{40}H_{32}N_8ClO_4Cu$: C, 56.8; H, 3.9; N, 13.9; Cu, 7.9%. [Cu(β-NaiMe)$_2$](ClO$_4$) (**3a**): *Anal.* Found: C, 52.2; H, 3.8; N, 17.6; Cu, 10.0. Calc. for $C_{28}H_{24}N_8ClO_4$ Cu: C, 51.9; H, 3.5; N, 17.1; Cu, 9.9%. [Cu(β-NaiEt)$_2$](ClO$_4$) (**3b**): *Anal.* Found: C, 54.3; H, 4.2; N, 16.9; Cu, 9.6. Calc. for $C_{30}H_{28}N_8ClO_4Cu$: C, 53.6; H, 4.0; N, 16.5, Cu, 9.4%. [Cu(β-NaiBz)$_2$](ClO$_4$) (**3c**): *Anal.* Found: C, 57.01; H, 4.1; N, 14.2; Cu, 8.1. Calc. for $C_{40}H_{32}N_8ClO_4Cu$: C, 56.9; H, 4.0; N, 14.0; Cu, 7.9%.

2.4. X-ray crystal structure analyses

Single crystals suitable for X-ray work of **1** were grown by slow evaporation of a methanolic solution of the synthetic mixture of [Cu(MeCN)$_4$][ClO$_4$] and 1-methyl-2-(phenylazo)imidazole (PaiMe) (1:2 mol ratio of metal ion and ligand) in a nitrogen chamber where a gentle stream of nitrogen gas is passed at ambient condition, while **2b** was grown by slow diffusion of hexane into a dichloromethane solution of the complex at 298 K. The suitable single crystals of the title complexes for X-ray analysis were mounted on a Siemens SMART CCD diffractometer equipped with a graphite monochromator and Mo Kα ($\lambda = 0.71073$ Å) radiation. Diffraction data for crystal **1** were measured using the ω-scan method. A summary of the crystallographic data and structure refinement parameters is given in Table 1. The intensity data were corrected for Lorentz and polarisation effects and an empirical absorption correction was employed using the SAINT [24] program for crystal **2b**. The structure was solved by the Patterson method using SHELXS-97 [25] followed by Fourier and difference Fourier synthesis for **2b** and a direct method was used to solve structure **1**. Full matrix least-squares refinements on F^2 were carried out using SHELXL-97 with anisotropic displacement parameters for all non-hydrogen atoms. The hydrogen atoms were fixed geometrically and refined using a riding model. In the final difference Fourier map the residual maxima and minima were 0.52 and −0.38 e Å^{-3}. All calculations were carried out using SHELXL-97, ORTEP-32 [26], PLATON [27] programs.

Table 1
Summarised crystallography data for [Cu(PaiMe)$_2$][ClO$_4$] (**1**) and [Cu(α-NaiEt)$_2$][ClO$_4$] (**2b**)

	1	**2b**
Empirical formula	$C_{20}H_{20}N_8ClO_4Cu$	$C_{30}H_{28}N_8ClO_4Cu$
Formula weight	535.43	663.59
Crystal size (mm)	0.60 × 0.28 × 0.16	0.40 × 0.30 × 0.20
Crystal system	monoclinic	tetragonal
Space group	$P2_1/n$	$P\bar{4}n2$
a (Å)	16.0380(2)	16.4294(13)
b (Å)	7.4892(1)	16.4294(13)
c (Å)	19.2186(1)	22.686(2)
β (°)	105.203(1)	90
Z	4	8
V (Å^3)	2227.60(4)	6123.50(9)
λ (Å)	0.71073	0.71073
ρ_{calc} (Mg m^{-3})	1.597	1.440
2θ Range (°)	3–55	3–56
T (K)	183(2)	293(2)
μ (Mo Kα) (mm^{-1})	1.147	0.850
Number of reflections	14417	36184
Unique reflections	4857	36184
Observed reflections ($I > 2\sigma(I)$)	3178	8967
Refined parameters	309	397
R	0.0526	0.0694
wR	0.1226	0.1502
Goodness-of-fit	0.94	0.74

[a] $R = \Sigma|F_o - F_c|/\Sigma F_o$. [b] $wR = [\Sigma w(F_o^2 - F_c^2)/\Sigma wF_o^4]^{1/2}$, where w is weighting factor. $w = 1/[\sigma^2(F_o^2) + (xP)^2]$; $x = 0.0520$ for **1** and 0.0665 for **2b** where, $P = (F_o^2 + 2F_c^2)/3$.

3. Result and discussion

3.1. Synthesis and spectral properties

The synthesis and structural formulation of copper(I) complexes with 1-methyl-2-(phenylazo)imidazole (PaiMe) have been reported by us [21]. It has been established by microanalytical and ^{1}H NMR spectral data that the complexes are bis-chelated copper(I), [Cu(PaiMe)$_2$]$^+$. Redox studies by cyclic voltammetry establish the stabilisation of the copper(I) complexes [Cu(II)/Cu(I), $E_{1/2} = 0.4$–0.5 V vs. SCE]. Monovalent copper(I) (d^{10}) complexes are usually unstable unless there is a neighbouring agency to stabilise the oxidation state. π-Acidic ligands in general and the azoimine function, −N=N−C=N−, in particular are an essential prerequisite for the stability of copper(I) complexes. The solution electronic spectra of the complexes exhibit high intense charge transfer transitions in the visible region (700–715, 560–570 nm) which are assigned to Cu(I) (dπ) → ligand (π*) (MLCT).

Bis-chelated 1-alkyl-2-(naphthyl-(α/β)-azo)imidazole (α/β-NaiR) complexes of copper(I), [Cu(α/β-NaiR)$_2$][ClO$_4$] have been isolated following a known procedure [21,22]. They are abbreviated as [Cu(α-NaiR)$_2$][ClO$_4$] (**2**) and [Cu(β-NaiR)$_2$][ClO$_4$] (**3**) (R = Me (**a**), Et (**b**), CH$_2$Ph(**c**)). The solution electrical conductivity supports the 1:1 electrolytic nature of the complexes in methanol. Infrared spectra of the complexes exhibit an intense band at approximately 1090 cm^{-1} along with a weak band at 625 cm^{-1} and have been assigned to ν(ClO$_4^-$). The ν(N=N) and ν(C=N) appear at 1390–1395 and 1570–1580 cm^{-1}, respectively, for **2** and **3**. In the free ligand, NaiR, they appear at 1400–1405 and 1595–1600 cm^{-1}, respectively. It is noticeable that ν(N=N) exhibits insignificant shifting to a lower energy region with respect to free ligand values compared with other copper(I)–arylazoheterocycles

[21]. This supports the weaker interaction between Cu(I) and N(azo) in $Cu(NaiR)_2^+$ than that of Cu(I)–{2-)(arylazo)pyridines/pyrimidines/imidazoles} complexes [21–23]. The solution electronic spectra of $Cu(NaiR)_2^+$ also exhibit a strong band around 400 nm ($\varepsilon \sim 10^4$) along with a weak band at longer wavelength, 485–505 nm ($\varepsilon \sim 10^3$) (Fig. 1). Free ligands also exhibit a strong intense absorption around 400 nm and thus the first band (~400 nm) may be assigned to an intraligand charge transfer transition. The weak band (Table 3, 485–505 nm) may be assigned to a MLCT transition. This is in contrast with reference to the reported Cu(I)–azoimine system [21–23] in which intense MLCT transitions appear at the red-region of the visible spectra, 650–750 nm. This transition is assigned to $d\pi(Cu) \rightarrow \pi^*(azo)$ of ligand and is associated with tetrahedral symmetry in the CuN_4 coordination sphere (Eq. (1)). Thus, we may conclude that Cu(I) in **2** and **3** does not follow tetrahedral symmetry which is also supported by the single crystal X-ray diffraction study (vide infra).

The ^1H NMR spectra of **2** and **3** were recorded in $CDCl_3$. The proton numbering pattern is shown in Scheme 1 and the spectral data are given in Table 3. The spectra have been compared with free ligand values and found that the signals are shifted to a higher frequency side. Imidazole protons 4- and 5-H, suffer maximum perturbation $\Delta\delta \sim 0.38$ ppm, difference in chemical shift data between free ligand and the present complex [17,18]. Naphthyl protons (7-H–13-H) suffer small perturbation ($\Delta\delta \sim 0.06$ ppm). The aliphatic region (< 6 ppm) shows a singlet signal for 1-Me at approximately 4.06 ppm for **2**. The methylene ($-CH_2-$) protons in $Cu(\alpha\text{-NaiCH}_2\text{CH}_3)_2^+$ and $Cu(\alpha\text{-NaiCH}_2\text{Ph})_2^+$ appear at 4.7 (quartet; $J = 12.0$ Hz) and 5.6 (singlet) ppm, respectively. A significant difference from the spectra of $Cu(\alpha\text{-NaiR})_2^+$ to $Cu(\beta\text{-NaiR})_2^+$ is the appearance of a singlet resonance at approximately 8.00 ppm which is assigned to 6-H in **3**. This observation also supports the preferential binding of Cu(I) with imidazole-N.

3.2. Molecular structure: tetrahedral versus linear geometry

3.2.1. Bis-[1-methyl-2-(phenylazo)imidazole]copper(I) perchlorate, $[Cu(PaiMe)_2](ClO_4)$ (1)

The molecular structure of **1** is shown in Fig. 2. Selective bond lengths and bond angles are given in Table 2. The central Cu(I) is coordinated by four N-donor centres (CuN_4 coordination) and is approximately tetrahedral symmetry. There are –N=N–C=N– chelation $[\overline{\text{Cu–(N=N–C=N}})\text{–}]$. The atomic groups Cu(1), N(1), N(2), C(7), N(4) and Cu(1), N(5), N(6), C(17), N(8) constitute two chelate planes (mean deviation, < 0.02 Å) and they make a dihedral angle of 87.6(4)°. The two chelate planes are distorted from T_d-symmetry and this deviation originates undoubtedly from the acute chelate bite angle. The chelate angles are N(1)–Cu(1)–N(4) 80.6(1)° and N(5)–Cu(1)–N(8) 80.3(1)°. The pendant phenyl ring is almost planar with the chelated azoimine fragment and the average dihedral angle is 6.5°. The two pendant phenyl rings are nearly orthogonal and make a dihedral angle of 86.3°. There are two different types of Cu–N bond lengths; i.e. Cu–N(imidazole) and Cu–N(azo) (Table 2). The Cu–

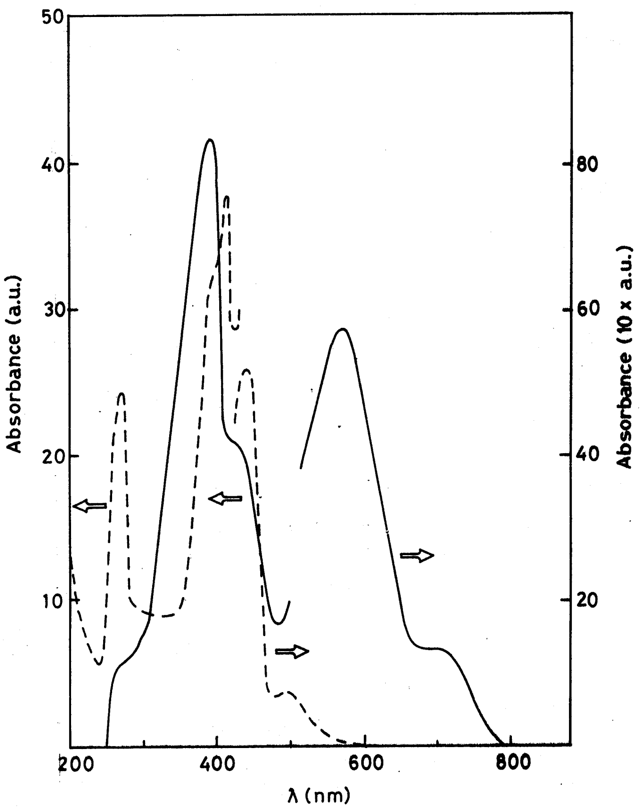

Fig. 1. UV–Vis spectral comparison of $[Cu(HaaiMe)_2](ClO_4)$ and $[Cu(\alpha\text{-NaiEt})_2](ClO_4)$ in MeOH.

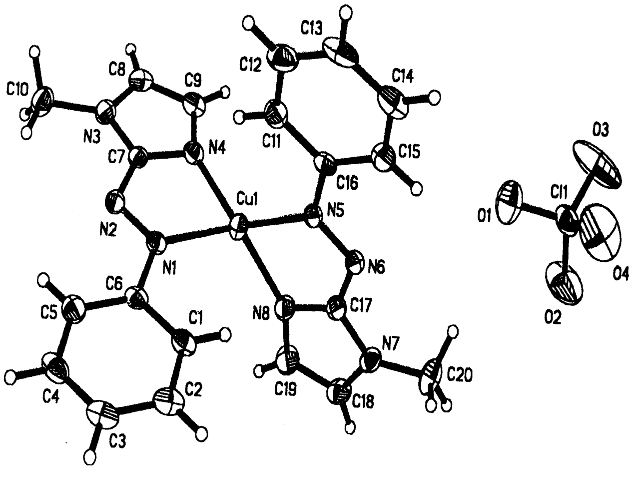

Fig. 2. X-ray structure of **1**.

Table 2
Selected bond distance (Å) and angles (°) for **1** and **2b**

	1	**2b**
Bond distances		
Cu(1)–N(1)	2.026(3)	2.686(6) [a]
Cu(1)–N(4)	2.006(3)	1.856(5)
Cu(1)–N(5)	2.015(3)	2.624(8) [a]
Cu(1)–N(8)	2.002(1)	1.846(5)
N(1)–N(2)	1.281(4)	1.266(5)
N(1)–C(6)	1.427(4)	1.433(7)
N(2)–C(7)	1.362(4)	1.395(9)
N(4)–C(9)	1.367(4)	1.386(6)
N(5)–N(6)	1.276(4)	1.278(6)
N(5)–C(16)	1.417(4)	1.388(8)
N(6)–C(17)	1.368(4)	1.402(7)
N(8)–C(17)	1.333(4)	1.364(7)
Bond angles		
N(1)···Cu(1)–(N4)	80.6(1)	69.9(1) [b]
N(1)–N(2)–C(7)	110.8(3)	112.0(5)
C(7)–N(4)Cu–(1)	106.5(2)	124.4(5)
N(5)···Cu(1)–N(8)	80.3(1)	71.6(0) [b]
N(5)–N(6)–C(17)	110.1(3)	112.9(6)
C(17)–N(8)–Cu(1)	106.8(2)	123.8(5)
N(1)–Cu(1)–N(5)	119.1(1)	75.6(1)
N(4)–Cu(1)–N(8)	129.7(1)	167.0(3)
N(1)–Cu(1)–N(8)	122.5(1)	121.2(5)
N(5)–Cu(1)–N(4)	130.4(1)	119.9(0)

[a] Cu···N(1)/N(5) weakly interacted bond.
[b] Forced chelate angles.

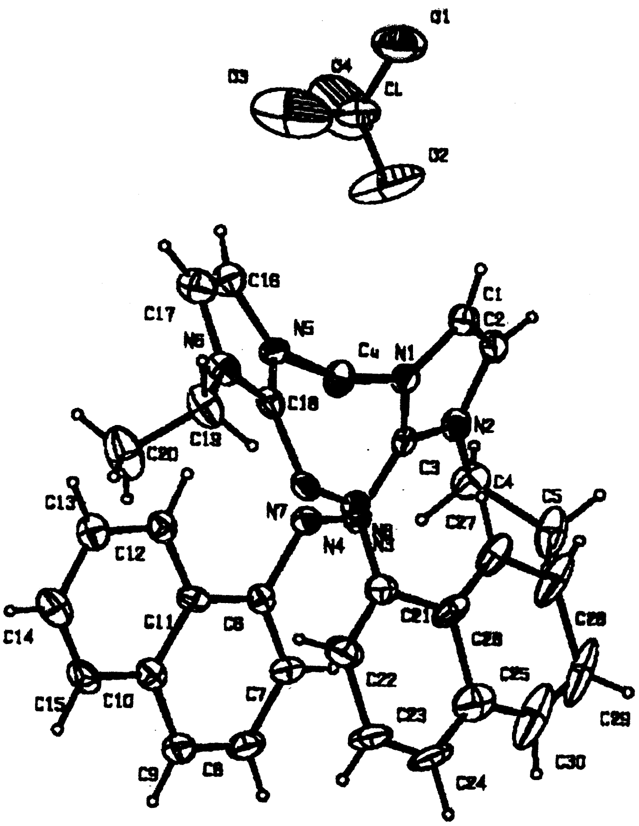

Fig. 3. X-ray structure of **2b**.

N(imidazole) bonds are shortened by 0.02 Å than the Cu–N(azo) bonds. The N=N bond distances are not equivalent in the two chelated fragments: N(1)–N(2), 1.281(4) and N(5)–N(6), 1.276(4) Å. In the free ligand the N=N bond lengths is 1.250(1) Å [28,29]. The elongation of the bond length supports the charge delocalisation from Cu(I) to ligand and is localised on the azo bond [22].

3.2.2. Bis-[1-ethyl-2-(naphthyl-α-azo)imidazole]copper(I) perchlorate, [Cu(α-NaiEt)$_2$](ClO$_4$) (2b)

The molecular structure of **2b** is shown Fig. 3 with bond lengths and angles being given in Table 2. The molecule shows a two coordinated CuN$_2$ linear geometry around copper(I) along with a distortion towards tetrahedral symmetry. There are four N-donor centres: two N(imidazole), N(4) and N(8), and two N(azo), N(1) and N(5), in the two coordinated α-NaiEt units. Each α-NaiEt can form a five membered chelate ring on coordination with the metal ion. The bond lengths show that N(imidazole) prefers to bind Cu(I) rather than N(azo) (vide supra). The Cu–N(imidazole) and short contact Cu···N(azo) distances are listed in Table 2. This is also supported by preferential binding of copper to imidazole-N in copper–metalloproteins [30]. The N=N distances in the two α-NaiEt units in **2b** are comparable with that of the N=N bond distance in the free ligand [1.267(3) Å] [20]. The sum of the van der Waals radii of Cu(I) and N(sp^2) is significantly greater than the Cu···N(azo) interaction distance [31] and warrants to consider that some short of bonding interaction exists between Cu(I) and N(azo). However, the comparison with the results of **1** is surprisingly different (vide infra).

The naphthyl and two imidazole rings make a dihedral angle of 16.97(3)° and 128.25(5)°, respectively. They markedly deviate from tetrahedral symmetry and are closer to a linear geometry. The forced chelate angles N(l)–Cu(l)···N(4), 69.9(1)° and N(5)–Cu(1)···N(8), 71.6(0)° are the lowest in the family of complexes of naphthylazoimidazoles of Pd(II) [15], Pt(II) [17] Ru(II) [18] and Os(II) [19] and in the series of the Cu(azoimine)$_2^+$-system where azoimine belongs to 2-(phenylazo)pyrimidine [22], and 1-methyl-2-(phenylazo)imidazole (vide infra). Thus, **2b** neither belongs to perfectly tetrahedral nor linear geometry and may be considered as [2+2] distorted linear geometry.

The bond lengths and angles in **1** and **2b** (Table 2) are not comparable although both the ligands belong to the azoimine (–N=N–C=N–) family with the phenyl group in **1** being substituted by a naphthyl group in **2**. The Cu–N(imidazole) bond length is shortened by approximately 0.15 Å in **2b** from that of **1**. Diagonally opposite behaviour is observed in the Cu–N(azo) distances. In **1**, the Cu–N(azo) bond length is comparable with reported results [22] while in **2b** these bond lengths (av. 2.65 Å) are exceptionally elongated by > 0.6 Å.

The chelate angle, being around 80.5° in **1**, are severely reduced (av. 70°) in **2b**. Larger steric interaction provided by two naphthyl groups of coordinated α-NaiEt in **2b** and higher electron donating ability compared with the phenyl ring in **1** may be the reasons for severe structural distortion from tetrahedral to linear geometry.

This is in contrast with Pd(II) [15], Pt(II) [17], Ru(II) [18], Os(II) [19] complexes of naphthylazoimidazoles. In these complexes the M–N(azo) bonds are shorter than M–N(imidazole) distances and consequently the N=N distance is elongated by 0.03–0.05 Å compared with free ligand values. In comparison with the 2-(phenylazo)pyrimidine Cu(I) complex [22], the Cu–N(azo) bonds are unusually elongated in **2b**. This deviation originates from the steric repulsion between the two naphthyl groups. The deviation from normal five membered chelate angles may cause severe distortion from tetrahedral geometry. The N(4)–Cu(1)–N(8) angle in **2b** is also deviated from tetrahedral as well a linear geometry; whereas the angles N(1)–Cu(1)–N(8) and N(5)–Cu(1)–N(4) are close to tetrahedral angles. Thus, we may conclude that the molecule is closer to linear geometry around Cu(I) having a weak interaction with the azo-N conforming to tetragonal distortion, i.e. a [2+2] distorted linear geometry.

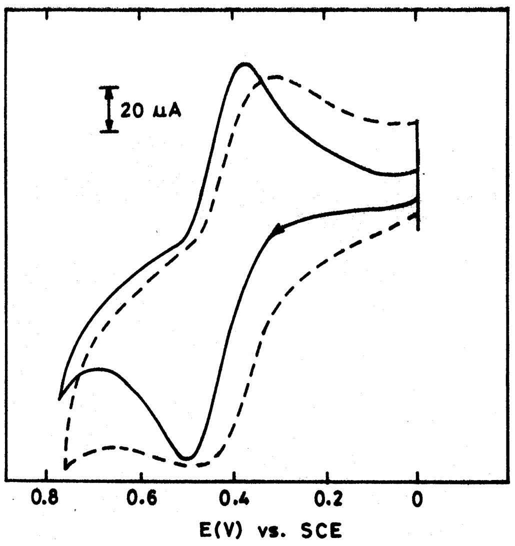

Fig. 4. Cyclic voltammetric comparison of $[\mathrm{Cu(HaaiMe)_2}](\mathrm{ClO_4})$ and $[\mathrm{Cu(\alpha\text{-}NaiEt)_2}](\mathrm{ClO_4})$ in MeOH–$\mathrm{CH_2Cl_2}$ using Pt-milli electrode, SCE as reference and Pt-wire auxiliary electrode; $[n\mathrm{Bu_4N}][\mathrm{ClO_4}]$ is the supporting electrolyte and solution concentration $\sim 10^{-3}$ M.

3.3. Redox properties

Redox properties of the complexes were examined by cyclic voltametry using a Pt-disk working electrode and a Pt-wire auxiliary electrode in dry MeOH–$\mathrm{CH_2Cl_2}$ (1:1, v/v) and in the presence of $[n\mathrm{BuN}^+][\mathrm{ClO_4}^-]$ as a supporting electrolyte. The potentials (Table 3, Fig. 4) are expressed with reference to the saturated calomel electrode (SCE) and uncorrected for junction potential. The complexes exhibit three redox couples, one couple positive to SCE and a pair of couples negative to SCE (Table 3). The redox response positive to SCE is quasireversible in nature as it is evident from $\Delta E_p >$ 100 mV and is assigned to the $\mathrm{Cu(NaiR)_2^{2+}}$/$\mathrm{Cu(NaiR)_2^{+}}$ (Eq. (1)) couple.

$$\mathrm{Cu(NaiR)_2^{2+}} + \mathrm{e} \rightleftharpoons \mathrm{Cu(NaiR)_2^{+}} \qquad (1)$$

Copper(I) complexes are usually unstable in air unless π-acidic ligands are coordinated to stabilise Cu(I) via a M → L charge transfer process. The azoimine function (–N=N–C=N–) being a good π-acceptor can stabilise a low valent metal redox state. Metal-redox potential data depend on the efficiency of the azoimine function, which has been controlled by the nature of the heterocycle, steric crowding, substituents type etc. Azopyridines are better π-acidic agents than azoimidazoles since five membered heterocycles are better π-donors and weaker π-acceptors than six membered heterocycles [16]. Thus Cu(I)–azopyrimidine complexes [22] show a higher Cu(II)/Cu(I) potential than that of the Cu(I)–azoimidazole derivative [23]. Compound **2b** shows relatively

Table 3
UV–Vis spectral and electrochemical data for **2** and **3**

Compounds	UV–Vis data λ_{max} (nm) [ε ($\mathrm{dm^3\ mol^{-1}\ cm^{-1}}$)]	Electrochemical data	
		E^{Cu}	$-E^{\mathrm{L}}$
$\mathrm{Cu(\alpha\text{-}NaiMe)_2ClO_4}$	490(385) [a], 452(7684), 412(12 400), 350(7357)	0.370(112)	0.909(165), 0.518(140)
$\mathrm{Cu(\alpha\text{-}NaiEt)_2ClO_4}$	1052(410), 450(8717), 416(11 541), 402(11 261), 352(7491) [a]	0.403(124)	0.499(353), 0.849(258)
$\mathrm{Cu(\alpha\text{-}NaiBz)_2ClO_4}$	485(400), 448(8642), 418(10 872), 400(11 202), 350(6747) [a]	0.426(198)	0.426(256), 0.840(260)
$\mathrm{Cu(\beta\text{-}NaiMe)_2ClO_4}$	500(420), 458 (8440), 392(11 350), 350(6997) [a]	0.731(117)	0.403(130), 0.567(140)
$\mathrm{Cu(\beta\text{-}NaiEt)_2ClO_4}$	504(425), 456(8614), 412(11 309), 352(7427) [a]	0.705(120)	0.415(120), 0.580(112)
$\mathrm{Cu(\beta\text{-}NaiBz)_2ClO_4}$	490(440), 448(8417), 412(12 023), 400(11 987), 352(6949) [a]	0.745(130)	0.394(127), 0.577(130)

Solvent MeOH–$\mathrm{CH_2Cl_2}$ (1:1, v/v).
[a] Shoulder.

low Cu(II)/Cu(I) potential values ($E_{1/2} \sim 0.4$ V vs. SCE) with respect to complexes of 1-alkyl-2-(arylazo)imidazoles ($E_{1/2} \sim 0.6$ V vs. SCE) (Fig. 4). It may be due to a sterically crowded, better electron donor napthyl group in Cu(NaiR)$_2^+$ than that of the aryl group in Cu(arylazoimidazole)$_2^+$. Besides, the structural distortion from T_d in Cu(PaiMe)$_2^+$ to linear in Cu(NaiR)$_2^{+2}$ may reduce the efficiency of retro-bonding (dπ(Cu) → π*(ligand)) phenomena. One electron stoichiometry of the complexes has been verified by bulk electrolysis (η = Q/Q/ = 0.96) for **2a** at potential 0.6 V versus SCE. The two redox couples negative to SCE (−0.5 to −0.6 and 0.7 to −0.9 V) are referred to azo reductions on comparing with the literature report [13].

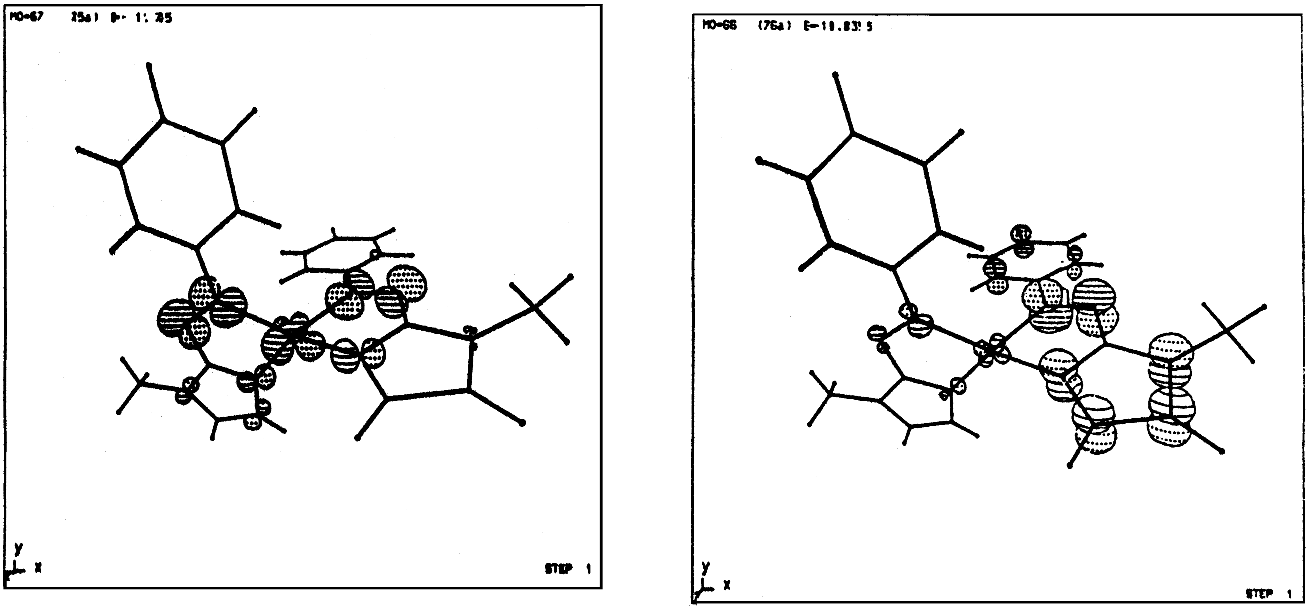

HOMO (a)

LUMO (a)

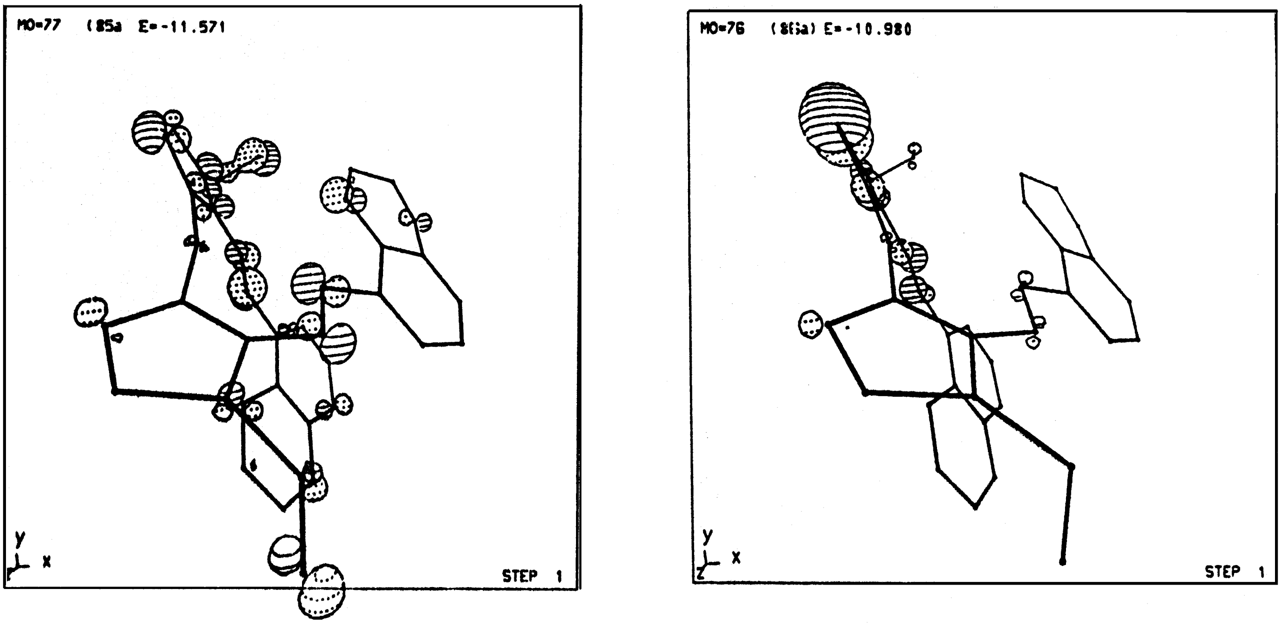

HOMO (b)

LUMO (b)

Fig. 5. HOMO and LUMO (a) Cu(HaaiMe)$_2^+$ (b) Cu(α-NaiEt)$_2^+$.

3.4. EHMO calculation and correlation with spectral/redox properties

In order to get an insight into the electronic properties of copper(I)–arylazoimidazoles and to explain their spectral and redox properties, MO calculations have been performed in the framework, of extended Huckel formalism. Crystallographic data of **1** was used for the EHMO calculation. The MOs are shown in Fig. 5 and relative percent atomic contribution to the MOs are given in Table 4. The HOMO (67) is contributed from 27.5% copper(I) [pπ 12%, dπ 15%] (FRG 2) and 72% ligand orbitals (FRG1). Other low-lying filled MOs (HOMO-1, HOMO-2) have been constituted from a major share of metal orbital. The LUMO(66) is characterised FRGI with 91% contribution from ligand orbitals.

In the case of **2b**, the HOMO(77) is 100% from the ligand, out of which azo (N=N), contributes 27.9%; N–Et imidazole, 52.93% and naphthyl group, 19.11%. There is no contribution of the orbitals from Cu. The LUMO(76) is also 100% contributed from the ligand, but the imidazole wave function predominates and is 93.02%; the azo function contributes 6.97% character and there is no naphthyl group contribution. From this EHMO calculation it is clear that there is no question of M → Ligand charge transfer and only the possibility of intra-ligand charge transfer (between imidazole and naphthyl group). This is also supported by UV–Vis spectral data.

Now some experimental findings can be rationalised on the basis of the EHMO results. In $Cu(PaiMe)_2^+$ the azoimine chelates (–N=N–C=N–) are involved in charge delocalisation which helps to stabilise the oxidation state while in $Cu(NaiR)_2^+$ only the imine function participates, [Cu–(N=C)–]. This has been proved by a higher $E_{1/2}$(Cu(II)/Cu(I)) in **1** than those in **2** or **3** by ~ 0.25 V. Because of the involvement of the azo group in the chelated system, **1** shows MLCT transitions in the longer wavelength region compared with those of **2** or **3**.

Table 4
Relative percentage of atomic contribution of the MOs of **2b** along with those of **1**

	HOMO		LUMO	
	2b	**1**	**2b**	**1**
Energy (eV)	−11.571	−11.705	−10.980	−10.835
Metal orbitals	0	27.5	0	0
Azo orbitals	27.9	62.5	8.54	60.24
Imidazole ring	52.93	10.0	91.46	31.33
Naphthyl/(phenyl)	19.11	0	0	8.43

4. Supplementary data

Crystallographic data for the structural analyses have been deposited with the Cambridge Crystallographic Data Centre, CCDC No. 186912 and 186232 for compound **1** and **2b**, respectively. Copies of this information may be obtained free of charge from The Director CCDC, 12 Union Road, Cambridge, CB2 1EZ, UK (fax: +44-1223-336033; e-mail: deposit@ccdc.ac.uk or www: http://www.ccdc.cam.ac.uk).

Acknowledgements

Financial assistance from the Department of Science and Technology, New Delhi is gratefully acknowledged. One of us (U.S.R.) thanks the University Grants Commission, New Delhi for giving a fellowship.

References

[1] T.A. Albright, J.K. Burdelt, M.-H. Whangbo, Orbital Interactions in Chemistry, Wiley, New York, 1984.
[2] R. Hoffmann, in: K.J. Laidler (Ed.), Frontiers of Chemistry, Pergamon Press, New York, 1982, pp. 247–263.
[3] F.A. Cotton, Chemical Applications of Group Theory, 3rd ed, Wiley, New York, 1999.
[4] W. Grochala, R. Hoffmann, Angew. Chem. Int. Ed. 40 (2001) 2742.
[5] W. Grochala, R. Konecny, R. Hoffmann, Chem. Phys. 265 (2001) 153.
[6] E.D. Jemmis, J. Am. Chem. Soc. 104 (1982) 7017.
[7] E.D. Jemmis, A.K. Phukan, U. Rosenthal, J. Organomet. Chem. 635 (2001) 204.
[8] V.W.W. Yam, B.W.K. Chu, C.C. Ko, K.K. Cheung, J. Chem. Soc., Dalton Trans. (2001) 1911.
[9] L. Gutierrez, G. Alzuet, J. Borras, M. Liu-Gonzalez, F. Sanz, A. Castineiras, Polyhedron 20 (2001) 703.
[10] F. Barriere, C.J. Pickett, J. Talarmin, Polyhedron 20 (2001) 27.
[11] D. Meilleur, P.D. Harvey, Can. J. Chem. 79 (2001) 552.
[12] C.K. Pal, S. Chattopadhyay, C. Sinha, A. Chakravorty, Inorg. Chem. 33 (1994) 6140.
[13] J.K. Nag, P.K. Santra, C. Sinha, F.-L. Lia, T.-H. Lu, Polyhedron 20 (2001) 2253.
[14] P.K. Santra, P. Byabartta, S. Chattopadhyay, L.R. Falvello, C. Sinha, Eur. J. Inorg. Chem. (2002) 1124.
[15] J. Dinda, D. Das, P.K. Santra, C. Sinha, L.R. Falvello, J. Organomet. Chem. 629 (2001) 28.
[16] E.C. Constable, Coord. Chem. Rev. 93 (1989) 205.
[17] S. Pal, D. Das, P. Chattopadhyay, C. Sinha, K. Panneerselvam, T.-H. Lu, Polyhedron 19 (2000) 1263.
[18] P. Byabartta, P.K. Santra, T.K. Misra, C. Sinha, C.H.L. Kennard, Polyhedron 20 (2001) 905.
[19] J. Dinda, S. Pal, B.K. Ghosh, J. Cheng, F.-L. Liao, T.-H. Lu, C. Sinha, J. Coord. Chem. (2002) in press.
[20] J. Dinda, K. Bag, C. Sinha, G. Mostafa, T.-H. Lu, Polyhedron (communicated).
[21] T.K. Misra, D. Das, C. Sinha, Polyhedron 16 (1997) 4163.
[22] P.K. Santra, D. Das, T.K. Misra, R. Roy, C. Sinha, S.-M. Peng, Polyhedron 18 (1999) 1909.

[23] D. Datta, A. Chakravorty, Inorg. Chem. 22 (1983) 1085.

[24] G.M. Sheldrick, SAINT, Ver. 5, Siemens Analytical X-ray Instrument, Inc., Madison, WI, 1995.

[25] G.M. Sheldrick, SHELXTL Software Reference Manual, Bruker AXS, Madison, WI, USA, 1997.

[26] L.J. Farrugia, ORTEP-3, J. Appl. Crystallogr. 30 (1997) 565.

[27] A.L. Spek, PLATON99, in: Molecular Geometry Program, University of Utrecht, The Netherlands, 1999.

[28] D. Das, Ph.D. Thesis, Burdwan University, Burdwan, India, 1998.

[29] A. Saha, C. Das, S. Goswami, S.-M. Peng, Indian J. Chem., Sect. A 40A (2001) 198.

[30] J.H. Schugar, in: K.D. Karlin, J. Zubieta (Eds.), Copper Coordination Chemistry, Biochemical Inorganic Perspectives, Ademine Press, New York, 1983.

[31] A.G. Orpen, L. Brammer, F.H. Allen, O. Kennard, D.G. Watson, R. Taylor, J. Chem. Soc., Dalton Trans (1989) SI.